IC/74/76
INTERNAL REPORT
(Limited distribution)

International Atomic Energy Agency

and

United Nations Educational Scientific and Cultural Organization

INTERNATIONAL CENTRE FOR THEORETICAL PHYSICS

T O P I C A L M E E T I N G

ON THE PHYSICS OF COLLIDING BEAMS

20 - 22 June 1974

(SUMMARIES AND CONTRIBUTIONS)

MIRAMARE - TRIESTE

July 1974

NEW RESULTS ON DEEPLY INELASTIC MUON-NUCLEON SCATTERING *

C.A. Heusch

Division of Natural Sciences II, University of California, Santa Cruz, Cal., USA.

ABSTRACT

We give a brief account of the experimental search for hadronic features of the virtual photon, as manifested in deeply inelastic muon-nucleon scattering. First results from the recent Santa Cruz-SLAC experiment are presented.

The remarkable scaling properties of electron-nucleon scattering phenomena, first postulated by Björken and subsequently investigated experimentally at SLAC and elsewhere, appear to hold up, at least approximately, in the much-extended kinematic regime opening up at NAL and then CERN SPS. This effect has yet to be explained in terms of individual channels that add up to the global behaviour exhibited by the data; also, first indications of a possible breakdown of scaling, claimed both at SLAC [1] and NAL energies [2], are perhaps small to make a fairly precise investigation of individual channels mandatory.

If we regard the 1-photon exchange mechanism as the only valid hadron production process, electron- and muon-nucleon interactions can be studied alternatively. Also, results will have to be interpretable, mutatis mutandis, together with the hadron production data of e^+e^- collisions.

Experiments studying the full final state have been very rare: only three to date.

1) $e^-p \to e^-$ + hadrons $E_e \leq 7.2$ GeV DESY
limited to $Q^2 \lesssim 1.5$, $\nu \lesssim 5$
streamer chamber allows for good data rate.

2) $\mu^-p \to \mu^-$ + hadrons $E_\mu \sim 1.5$ GeV SLAC Gp. A,B,C
limited by performance characteristics of bubble chamber used in a hybrid set-up;
only $\sim$ 500 events with $Q^2 > 0.5$.

3) $\mu^+ p \rightarrow \mu^+ +$ hadrons $\quad E_\mu \sim 14.2$ GeV UCSC-SLAC Gp. D
streamer chamber experiment. Marginal sensitivity to elastic or low Q^2 events. 10,000 deeply inelastic events ($Q^2 > 0.5$).

In addition, there are a number of limited solid-angle experiments that are sensitive to particular features of final-state hadron production. Experiments (1) and (2) have published results. We show here some first features of interest emerging from the Santa Cruz-SLAC experiment (3) above.

This experiment (SLAC E-72) based its promise on the building of an optimal muon beam. The cost of producing high-energy muons at an electron accelerator is high; in order to obtain our muon of 14.2 GeV in the phase space of our beam line, approximately 10^9 electrons had to be accelerated to 21 GeV. The pay-off comes when we compare the performance data of this beam:

$$E_\mu = 14.2 \text{ GeV}$$

$$I_\mu \leq 10^5 \text{ sec}^{-1}$$

$$\frac{\Delta p}{p} \approx \pm 1\%$$

$$\Delta\theta \approx \pm 2 \text{ m rad}$$

$$\text{beam spot} \approx 1 \text{ cm}^2$$

$$\text{halo} \approx 1\%$$

$$\pi \text{ contamination} \approx 4 \times 10^{-5}$$

with those obtained at proton machines. There, the beam spots are typically 10-100 times larger, and the halo usually contains up to one-half the total flux.

Fig.1 shows the experimental set-up; the muon beam traverses a 40 cm long liquid-hydrogen target located inside a 2m long streamer chamber. The whole system is immersed in a 16 k-Gauss magnetic field. Non-interacting muons exist through a beam pipe, and register in a Cherenkov flux monitor system accurate to this 1% level. Muons scattered out of the phase space of the beam will traverse a series of hodoscopes and wire chambers sandwiching a total hadron absorber thickness of 1.50 cm of lead. While this detection system is optimized for the scaling region ($Q^2 > 0.5$, $\nu > 2$), there are efficiency tails for elastic scattering and "shallow inelastic" events. Appropriate logic signals from hodoscope coincidences cause the streamer

chamber to fire and the event to be photographed in three views.

Since we run several hundred muons through the streamer chamber during its memory time, delta rays might constitute a severe problem. We minimize it by the insertion of teflon delta ray absorbers above and below the target as shown in Fig.2; we also place the entire target inside a re-entrant box filled with an inert gas. The ensuing loss of visual information very close to the vertex turned out not to present serious problems.

We present here first features emerging from a look at some 6,000 deeply inelastic events, amounting to about 40% of our data.

The first exclusive channel to be checked is the elastic one, $\mu^+ p \to \mu^+ p$. Fig.3 gives the data together with the "dipole" fit to ep scattering, weighted for our luminosity and detection efficiency. It is seen that the agreement is quite satisfactory. We expect our final data sample to allow for a 5% comparison between electron- and muon-proton elastic scattering.

We now look for properties of photon-hadron couplings that might exhibit telling differences between real and virtual photons. Figs.4 and 5 show fractional cross-sections for $\gamma_v p \to$ one, three, or five charged groups (neutrals are not detected). There are two striking features: while there is a significant s dependence in these cross-sections, none of the kinematic bins shown gives any indication for a Q^2 dependence. In other words, there is clearly no scaling in the individual and multiplicity channels. Second, the one-group cross-section is considerably higher <u>in all s bins</u> above s = 2 than what has been known in photoproduction ($Q^2 = 0$). Three-groups, conversely, are more abundant in photoproduction than in electroproduction, except in the lowest s bin. These features are understandable in terms of individual channels: one-groups contain $\gamma_v p \to \pi^+ n$, $\pi^0 p$, whereas the vector mesons are contained in the three-groups $\gamma_v p \to \rho^0 p$, $\omega^0 p$, $\phi^0 p$. Vector mesons, however, make up less and less of the axial inelastic cross-sections as Q^2 increases [3]. We are then faced with the remarkable fact that, while $\sigma_\rho / \sigma_{tot}$ <u>decreases</u> with Q^2 , this Q^2 dependence does <u>not</u> show up significantly in the one- and three-group fractional cross-sections once we move away from $Q^2 = 0$. Rather, some compensatory mechanism appears to be at work.

When we plot the mean charged multiplicity as a function of hadronic energy s , a good fit to the data (at $Q^2 \sim 1.4$) is (cf. Fig.6)

$$\langle n \rangle_{ch} = 0.7 + \ell n\, s \quad ,$$

where the slope is very close to that observed in photoproduction. This again indicates a cancelling out of individual channels in such a fashion as to make the increased presence of one-group mechanisms show up only in a vertical off-set of the $Q^2 > 0$ vs. the $Q^2 = 0$ line. This is in contradiction with the findings of a Cornell group [4], which reports a considerably steeper logarithmic multiplicity increase for virtual as opposed to real photoproduction. Another remarkable feature in this context is the increase with Q^2 of the preponderance of positive over negative particles in the forward direction. The trend is indicated in Fig.7 (from a limited data sample), where we show the charge ratio n_+/n_- for hadronic masses above the resonance region for all particles with fractional longitudinal momentum $x > 0.3$. Clearly, there is no leading particle effect associated with the (neutral) photon that would make us expect this feature.

In conclusion, we remark that some remarkable differences are showing up in hadron production of virtual vs. real photons:

1) $\sigma(1\text{-prong})_{Q^2 > 1} > \sigma(1\text{-prong})_{Q = 0}$ for all $s > 2$.

2) $\sigma(1, 3, 5\text{-}\cdots \text{ prong})$ appear to be independent of Q^2 for all energies.

3) $\sigma(1, 3, 5\text{-}\cdots \text{ prong})$ show strong energy dependence. No scaling.

4) $\langle n \rangle_{ch} \sim 0.7 + \ell n\, s$ (approximately like in $\bar{p}p$). Slope as in photoproduction (as opposed to Cornell data).

5) n_+/n_- increases significantly with Q^2, for forward hadrons and $W > 2.8$.

More detailed features will be reported shortly, at the forthcoming London conference.

REFERENCES

1) A. Bodek, MIT preprint (1973).

2) L. Hand, Seminar given at SLAC, May 1974.

3) UCSC-SLAC collaboration, Report to the London Conference, preprint UCSC 74/02.

4) B. Gibbard et al., Cornell preprint CLNS-266 (1974).

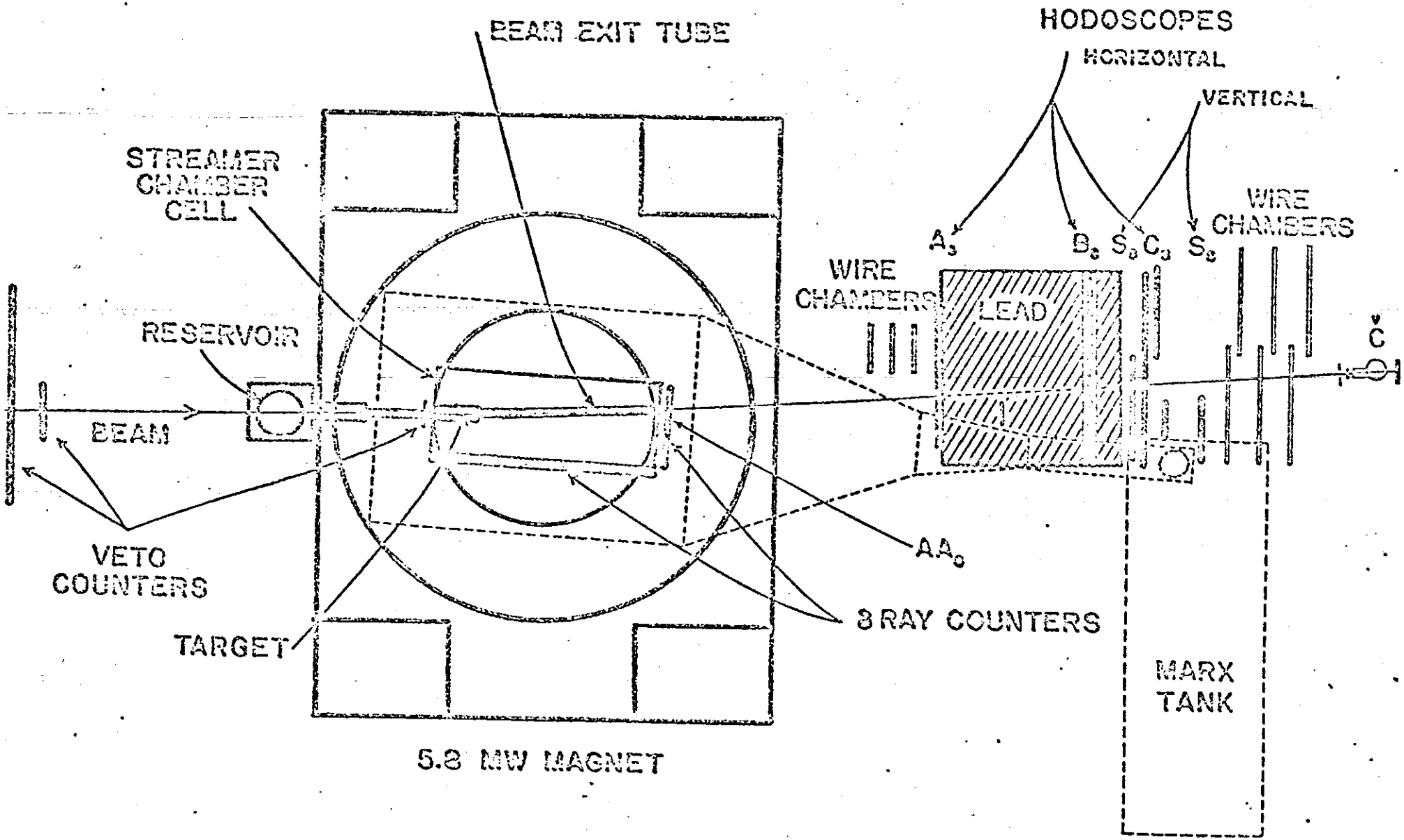
BEAM EXIT TUBE
HODOSCOPES
HORIZONTAL
VERTICAL
STREAMER CHAMBER CELL
WIRE CHAMBERS
A_3
B_3 S_3 C_3 S_3
WIRE CHAMBERS
LEAD
RESERVOIR
C
BEAM
VETO COUNTERS
AA_0
TARGET
β RAY COUNTERS
MARX TANK
5.8 MW MAGNET

Fig.1

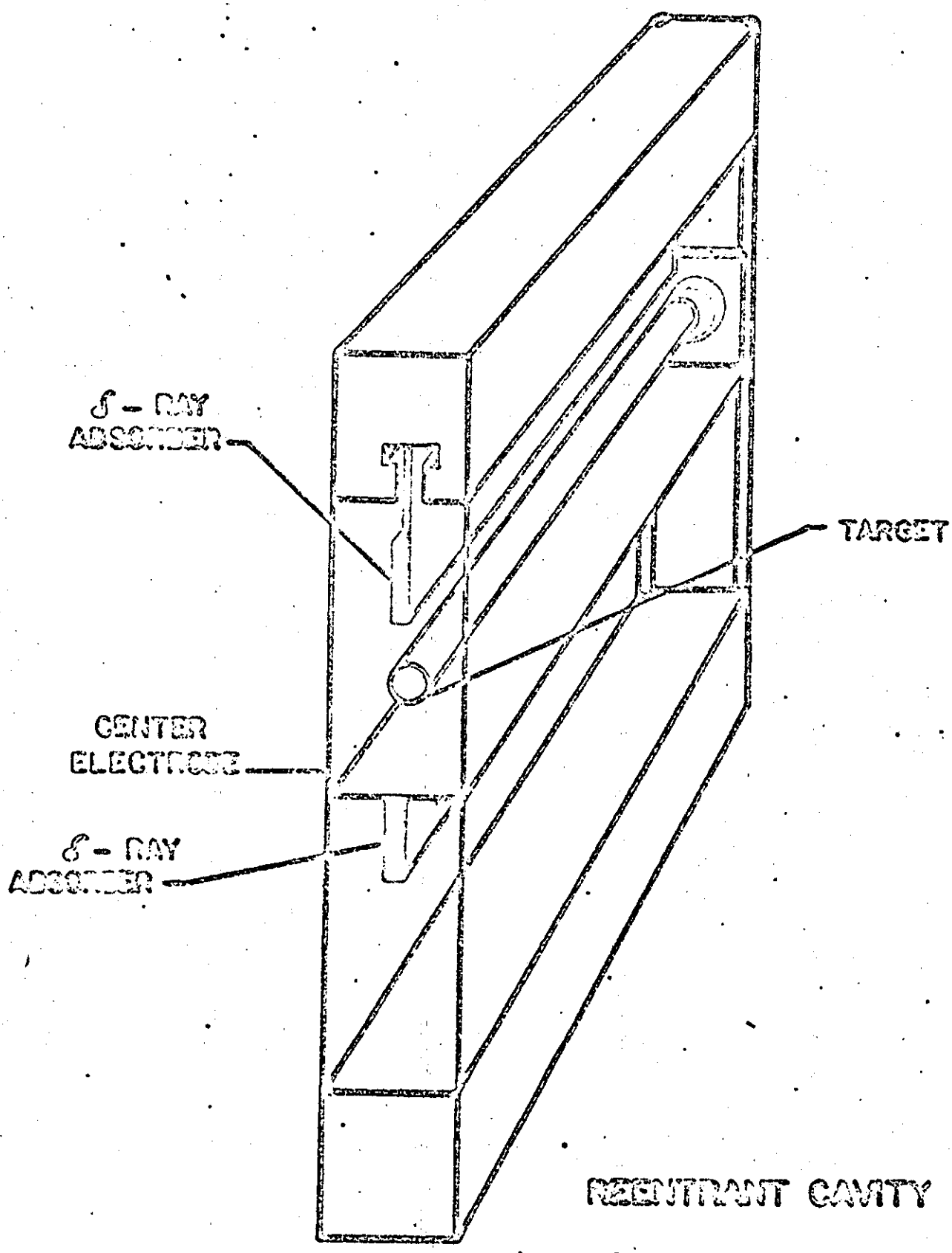
δ - RAY
ABSORBER
TARGET
CENTER
ELECTRODE
δ - RAY
ABSORBER
REENTRANT CAVITY

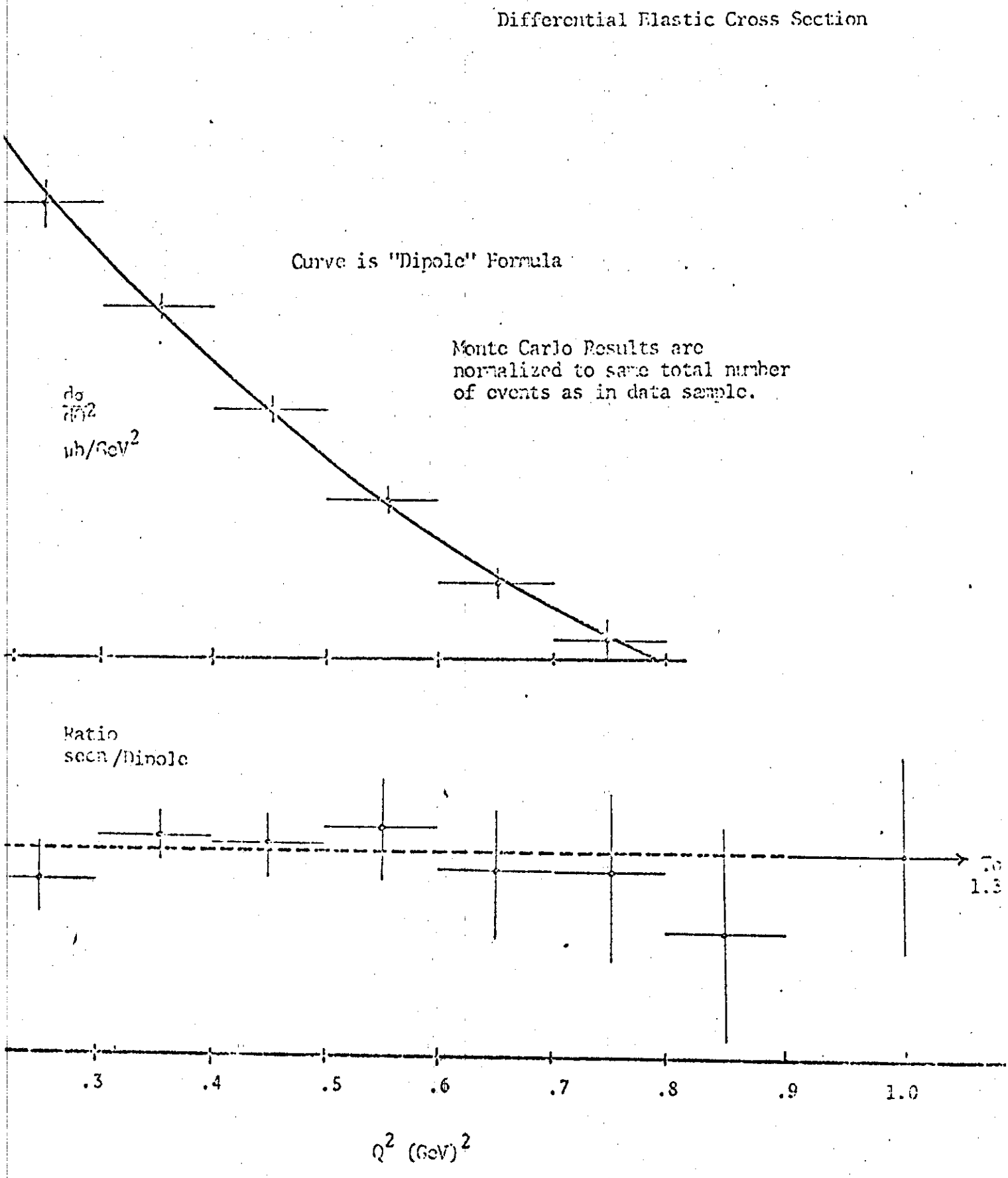
Differential Elastic Cross Section
Curve is "Dipole" Formula
Monte Carlo Results are normalized to same total number of events as in data sample.
dσ/dQ²
μb/GeV²
Ratio
seen/Dipole
1.3
.3
.4
.5
.6
.7
.8
.9
1.0
Q² (GeV)²

Fig.3

Fig.4

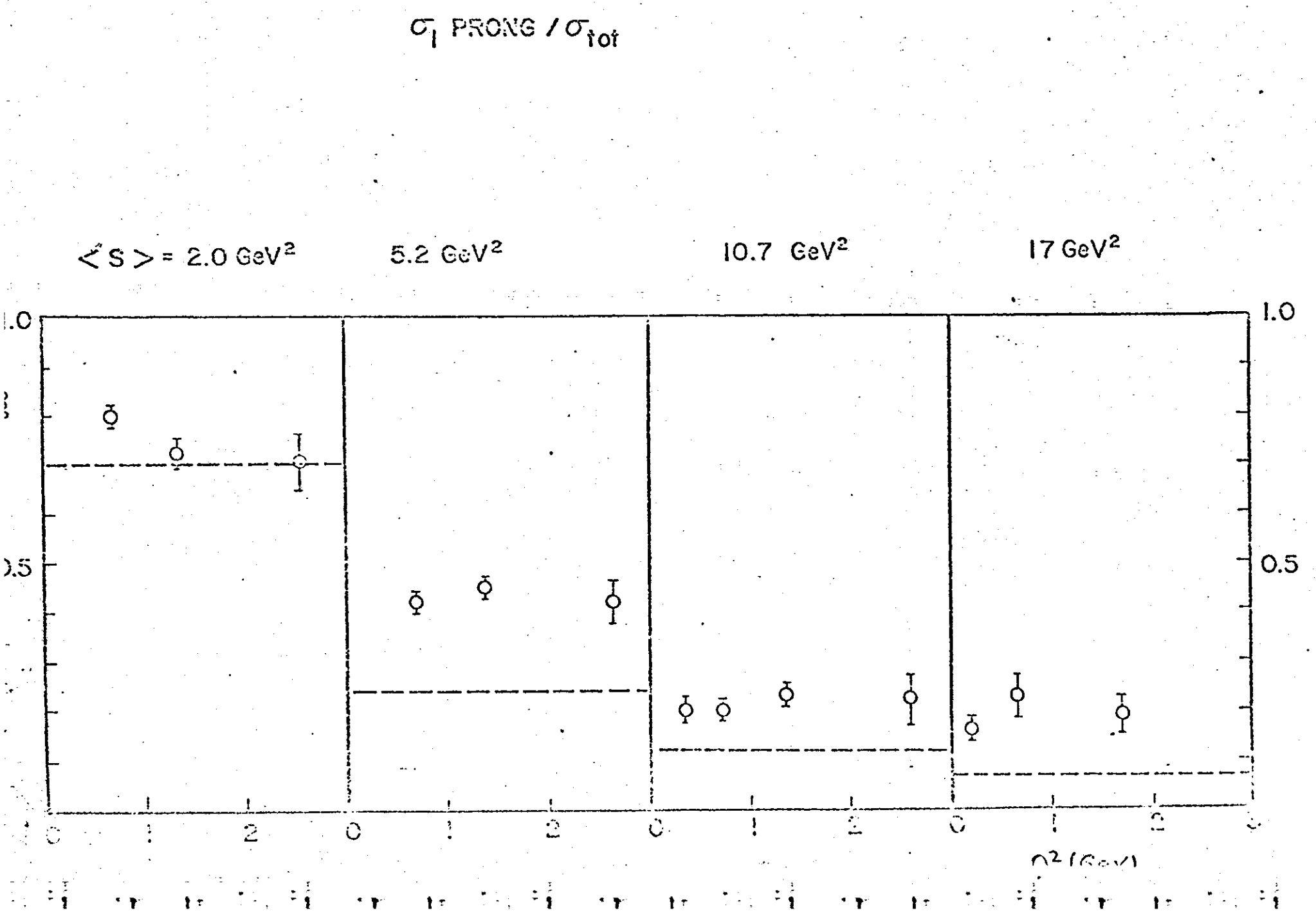
σ_1 PRONG / σ_{tot}
< S > = 2.0 GeV²
5.2 GeV²
10.7 GeV²
17 GeV²
1.0
0.5
0
1
2
Q² (GeV)

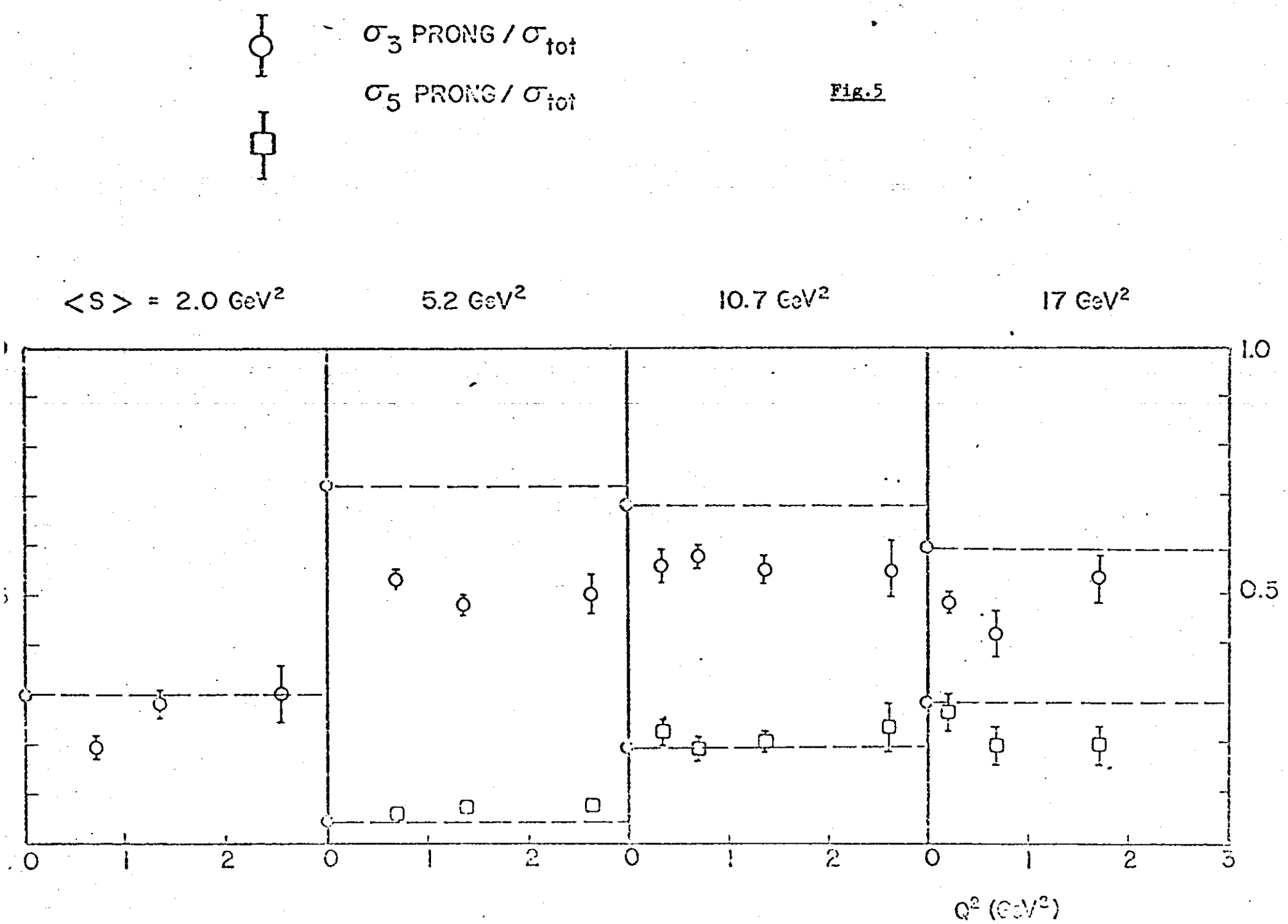
σ_3 PRONG / σ_{tot}
σ_5 PRONG / σ_{tot}
<S> = 2.0 GeV²
5.2 GeV²
10.7 GeV²
17 GeV²
1.0
0.5
0
1
2
0
1
2
0
1
2
0
1
2
3
Q² (GeV²)

Fig.5

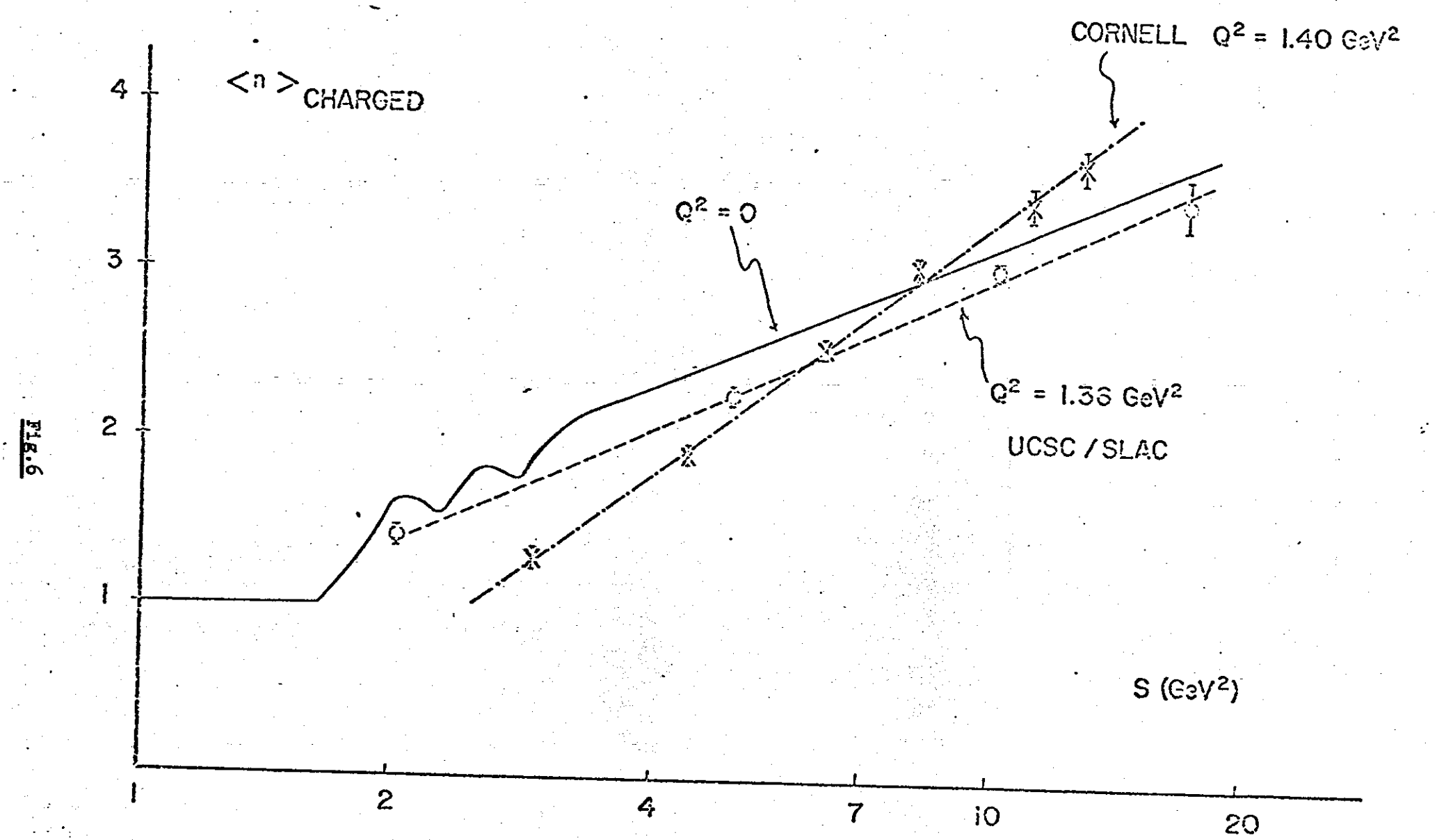
CORNELL Q^2 = 1.40 GeV²
$\langle n \rangle_{CHARGED}$
$Q^2 = 0$
Q^2 = 1.36 GeV²
UCSC / SLAC
S (GeV²)
4
3
2
1
1
2
4
7
10
20

Fig.6

Charge ratio for forward hadrons:

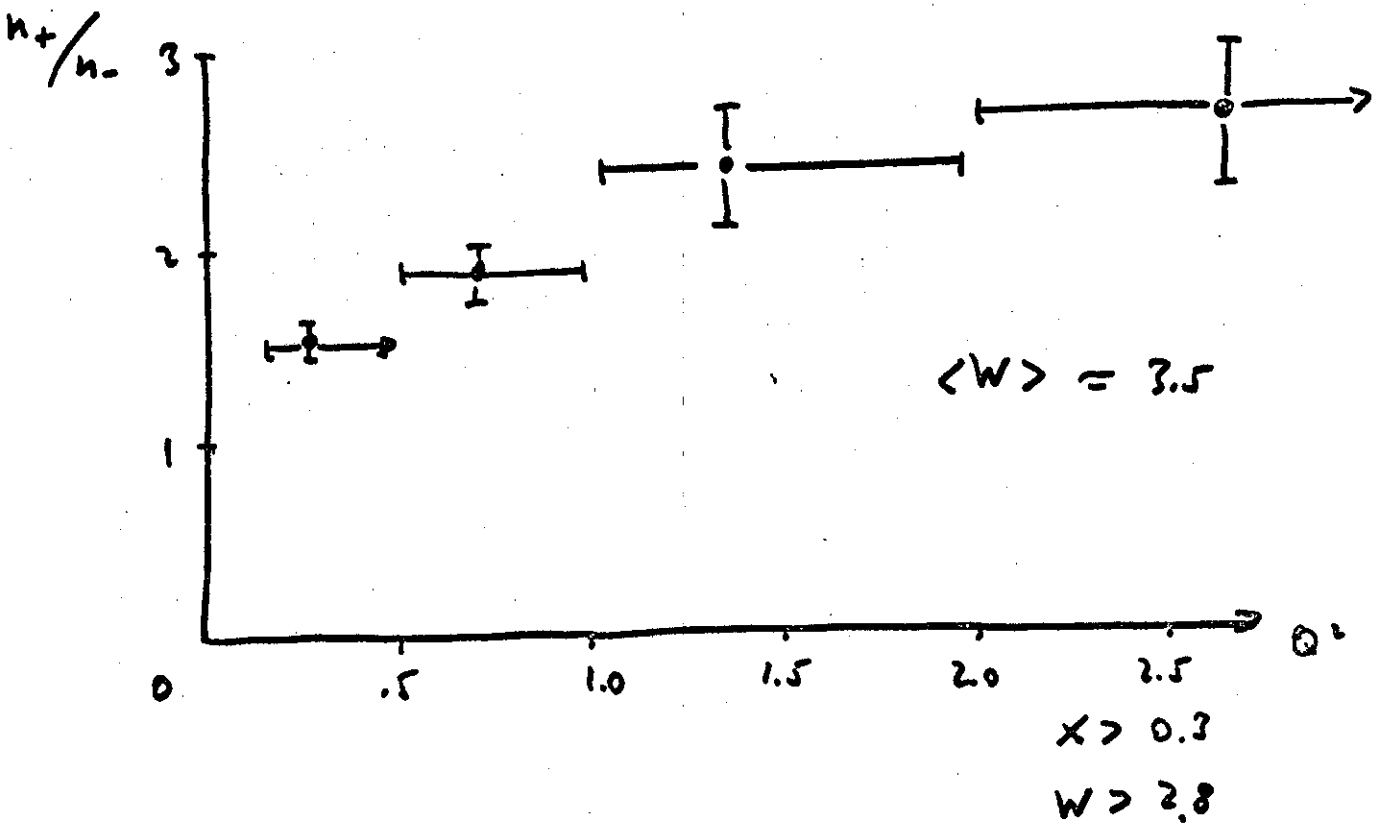

Fig.7